Title

Independent Poincaré-Sphere Analysis of Polarization States in Integrated Structured-Light Architectures

Author
Fakhimi, Alexa N

Publication Date
2025-12-11

Independent Poincaré-Sphere Analysis of Polarization States in Integrated Structured-Light Architectures

Alexa Fakhimi[1]

[1] *Electrical Engineering Undergraduate Student at the University of California, Los Angeles (UCLA)*
**alexafakhimi@g.ucla.edu*

Abstract: This paper discusses the polarization results reported by Lemons et al., using Stokes parameters and Poincaré-sphere mapping to evaluate the alternating linear, asymmetric linear, and asymmetric circular polarization states.

INTRODUCTION

Structured light, optical fields engineered in amplitude, phase, and polarization, has become central to modern applications in communication, sensing, microscopy, and strong-field science. Many of these rely on precise control of transverse polarization topology, which sets the beam's spin-angular-momentum structure. Conventional tools such as liquid-crystal SLMs can shape phase and amplitude, but they have limited power handling and cannot independently or dynamically control polarization, temporal phase, and pulse timing.

The paper introduced a coherent multi-channel fiber-array laser architecture that enables programmable control of amplitude, phase, polarization, and timing in each beamline. Their system can synthesize complex polarization and phase topographies at high peak power; in particular, their Figure 4 shows three spatial polarization patterns, alternating linear, asymmetric linear, and asymmetric circular, along with measured Stokes maps.

This review independently analyzes those polarization configurations. We reconstruct representative transverse polarization vectors from the reported near-field polarization patterns, compute the associated Stokes parameters, and map them onto the Poincaré-Sphere to assess the fidelity of the polarization synthesis.

METHODS

This review examines the polarization configurations shown in Figure 4 of the paper and evaluates them using standard polarization theory and numerical modeling. The analysis begins by identifying representative transverse polarization vectors $(E_x, E_y)^T$ associated with the alternating linear, asymmetric linear, and asymmetric circular patterns illustrated in the near-field diagrams. These complex field vectors serve as idealized models of the local polarization states generated by the multi-channel architecture.

For each representative polarization vector, the corresponding Stokes parameters were computed using their standard definitions:

$$S_0 = |E_x|^2 + |E_y|^2 \text{ (1)}, S_1 = |E_x|^2 - |E_y|^2 \text{ (2)}$$

$$S_2 = 2Re(E_x E_y^*) \text{ (3)}, S_3 = 2Im(E_x E_y^*) \text{ (4)}$$

The normalized Stokes vector

$$(s_1, s_2, s_3) = (S_1, S_2, S_3)/S_0 \quad (5)$$

provides a direct geometric representation of each state on the Poincaré-Sphere, where linear and circular polarizations occupy the equatorial and polar regions, respectively.

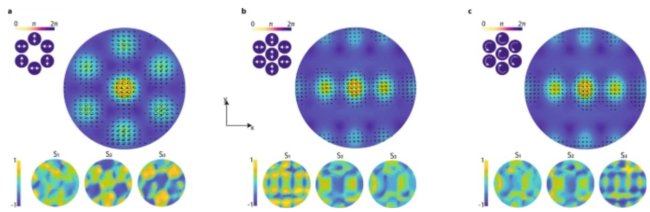

Fig. 4. Reproduced from Lemons et al. Experimental results of polarization topography evolution with corresponding near-field configurations (top left) and Stokes projections (bottom) for alternating linear (a), asymmetric linear (b), and asymmetric circular polarization coherent synthesis (c).

MATLAB was used to perform all calculations of the Stokes parameters and to generate the corresponding Poincaré-Sphere visualization.

The transverse polarization vectors for each configuration were input into MATLAB, which evaluated equations (1)-(5) and plotted the resulting normalized Stokes vectors. This numerical model produces the ideal Poincaré-Sphere locations for horizontal, vertical, diagonal, right-hand circular, and left-hand circular polarization. These ideal results were then compared qualitatively with the measured S_1, S_2, and S_3 maps shown in Figure 4 to assess the fidelity of the polarization synthesis.

This combined analytical and computational approach allows direct comparison between theoretical polarization states and the experimentally generated structured-light distributions.

RESULTS AND INTERPRETATION

The Jones vector representation provides the basis for computing the Stokes parameters used throughout this analysis. The idealized Stokes vectors computed for the representative polarization states provide a basis for evaluating the measured distributions shown in Figure 4. For the alternating linear configuration, the theoretical polarization vectors correspond to horizontal and vertical linear polarization, which map to (1, 0, 0) and (-1, 0, 0) on the Poincaré-Sphere. The experimental S_1 map exhibits alternating positive and negative regions consistent with this pattern, while the S_2 and S_3 maps are close to zero. This agreement indicates that the array successfully produces a spatial sequence of orthogonal linear polarization states.

The asymmetric linear configuration is modeled as a rotated linear polarization state with a representative polarization vector at 45°. Its ideal Stokes vector lies at (0, 1, 0) on the Poincaré equator. In the measured distribution, the S_2 projection displays strong positive and negative lobes, while the S_1 and S_3 components show lower magnitude. This behavior matches the characteristics of a diagonally oriented linear polarization and demonstrates the system's ability to generate non-orthogonal linear states across the array.

The asymmetric circular configuration is represented by left-hand and right-hand circular polarization, which occupy the north and south poles of the Poincaré sphere. The calculated Stokes vectors are (0, 0, 1) and (0, 0, -1). The experimental S_3 map shows distinct positive and negative regions corresponding to these poles, with relatively small contributions from S_1

and S_2. These results indicate that the architecture produces alternating handedness in the circular polarization distribution, consistent with the intended design.

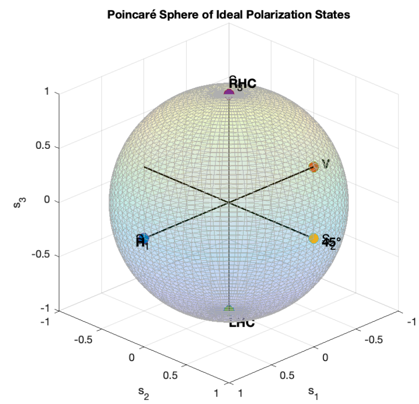

Fig. 5. *MATLAB-generated Poincaré-Sphere representation of the ideal polarization states corresponding to the three configurations shown in Figure 4. Horizontal, vertical, and diagonal linear polarization lie on the equator, while right-hand and left-hand circular polarization occupy the poles.*

Across all three configurations, the MATLAB-calculated Stokes vectors align with the qualitative structure of the measured polarization maps. Small deviations from the ideal patterns, such as residual S_2 components in nominally linear states or slight ellipticity in circular states, may arise from channel amplitude imbalance, imperfect phase matching, or alignment variations across the array. Nonetheless, the central features of each polarization configuration are preserved, indicating that the system achieves high-fidelity synthesis of spatially varying polarization topographies.

CONCLUSIONS

This review applied Stokes-parameter analysis and Poincaré-Sphere visualization to evaluate the polarization distributions presented in Figure 4 of the paper. Representative polarization vectors were used to calculate the ideal Stokes parameters for alternating linear, asymmetric linear, and asymmetric circular configurations, and MATLAB was used to generate the corresponding Poincaré-Sphere representation. Comparison between these ideal results and the measured Stokes maps demonstrates that the architecture produces the intended polarization states with good qualitative fidelity. Minor discrepancies between the ideal and experimental distributions can be attributed to amplitude imbalance, alignment tolerances, or other practical factors inherent to multi-channel coherent synthesis. Overall, the analysis confirms that the architecture provides effective spatial control of polarization and represents a viable approach for high-power structured-light generation. In future work, this approach may be extended to higher-order vector beams or applied to a quantitative analysis of error sources in the polarization-synthesis process.

REFERENCES

1. Lemons, R., Liu, W., Frisch, J.C. et al. Integrated structured light architectures. Sci Rep 11, 796 (2021). https://doi.org/10.1038/s41598-020-80502-y
2. Liu, Jia-Ming. Principles of photonics. Cambridge University Press, 2016.
3. Thorlabs Inc., "Using the Poincaré Sphere to Represent the Polarization State," (Sept. 11, 2020).
4. "Poincaré Sphere," *Fiber Optics 4 Sale Web Blog*, Apr. 25 2016, https://www.fiberoptics4sale.com/blogs/wave-optics/104501958-poincare-sphere